NF-κB participates in chemokine receptor 7-mediated cell survival in metastatic squamous cell carcinoma of the head and neck

FA-YU LIU[1], ZHEN-JIN ZHAO[1], PENG LI[1], XUE DING[1], NAN GUO[1], LIANG-LIANG YANG[1], ZHI-HONG ZONG[2] and CHANG-FU SUN[1]

[1]Department of Oromaxillofacial-Head and Neck Surgery, Department of Oral and Maxillofacial Surgery, School of Stomatology, China Medical University, No. 117, Nanjing Bei Jie, Heping District, Shenyang, Liaoning 110002; [2]Department of Biochemistry and Molecular Biology, China Medical University, No. 92, Beier Road, Heping District, Shenyang, Liaoning 110001, P.R. China

Received August 19, 2010; Accepted October 18, 2010

DOI: 10.3892/or.2010.1090

Abstract. Metastatic squamous cell carcinoma of the head and neck (SCCHN) has been shown to express chemokine receptor 7 (CCR7), which activates phosphoinositide-3 kinase/Akt/mammalian target of rapamycin (PI3K/Akt/mTOR) signal pathway to promote the invasion and survival of SCCHN cells. Since nuclear factor-kappa B (NF-κB) is shown to be the downstream signal molecule of PI3K/Akt in many tumors, we investigated whether it also exists in the CCR7 pathway in SCCHN, and the relationship between NF-κB and PI3K/Akt/mTOR, and the role it plays in SCCHN. We assayed the phosphorylation of the inhibitor of NF-κB (IκBα), the NF-κB DNA-binding capacity and location. The results showed that the interaction between CCR7 and the ligand for CCR7, CCL19, induces phosphorylation of IκBα, causes NF-κB to translocate to the nucleus and raises the DNA-binding capacity of NF-κB. The phosphorylation and DNA-binding capacity were abolished by the inhibition of CCR7, PI3K, Akt and mTOR. Further research demonstrated that inhibitors of NF-κB and CCR7-PI3K attenuate the survival of CCR7-mediated cells, causing decreased viability, increased apoptosis and increased cell cycle arrest in SCCHN cells. In clinical samples from 78 patients, immunohistochemical assay also showed that CCR7 and NF-κB are not only highly expressed in SCCHN, but also correlated with each other, and related to lymph node metastasis and clinical stage. Together, our data indicate that NF-κB is activated by CCR7 via PI3K/Akt/mTOR, and this signal pathway plays an important role in regulating the cell survival and prognosis of SCCHN.

Correspondence to: Dr Chang-Fu Sun, Department of Oromaxillofacial-Head and Neck Surgery, School of Stomatology, China Medical University, No. 117, Nanjing Bei Jie, Heping District, Shenyang, Liaoning 110002, P.R. China
E-mail: cfsun@mail.cmu.edu.cn

Key words: NF-κB, CCR7, PI3K, squamous cell carcinoma of head and neck, survival

Introduction

Chemokines are a group of small, structurally-related molecules that constitute a superfamily of inducible, secreted, proinflammatory proteins that are involved in a variety of immune responses (1-4). Chemokines are classified into four major groups based on the number and spacing of conserved cysteines: CXC, CC, C and CX3C. The CC chemokine receptor 7 (CCR7) has two ligands: CCL19 and CCL21. The interaction between CCR7 and its ligands promotes the migration, invasion and chemotaxis of T cells, B cells, natural killer cells (NK cells), mature dendritic cells (DC) and some tumors. The tumors affected by this interaction include: esophageal squamous cell carcinoma, colorectal carcinoma, non-small cell lung cancer, hepatocellular cancer, breast cancer, and melanoma (5-12).

Recently, a novel role for CCR7 was described in mesangial cells. CCR7 and its ligand, CCL21, may potentially be involved in proliferation, apoptosis, tissue homeostasis and adhesion in the kidney (13-15). Additionally, CCR7 activates signals that inhibit apoptosis of mature DCs and T lymphocytes through the phosphatidylinositol 3-kinase (PI3K)/Akt pathway (16,17). In metastatic SCCHN cell lines, CCR7 also prevented cell death by phosphorylation of Akt in a PI3K-dependent fashion (18-20). These studies indicate that CCR7 mediates cell survival by activating the PI3K/Akt pathway.

PI3K/Akt is a well-studied signaling pathway. We recently reported that in metastatic SCCHN cell lines, CCR7 activates the mammalian target of rapamycin (mTOR) signal by PI3K/Akt. This signal cascade plays a important role in CCL19-induced cell survival (21).

Aside from its effects on the mTOR signal, the PI3K/Akt signal pathway influences many other downstream molecules, including nuclear factor-kappa B (NF-κB). The mammalian NF-κB family consists of five members, p50, p52, p65/RelA, c-Rel, and RelB, which are tightly controlled by a family of inhibitory molecules (IκBs). This family comprises IκBα, IκBß, IκBε and the precursor molecules for p50 and p52,

p105 and p100, respectively. IκB proteins prevent nuclear entry and DNA binding of NF-κB (22). The Akt-induced activation of the IκB kinase (IKK) complex results in the phosphorylation of IκBs, which are subsequently degraded by the proteasome. The degradation of IκBs allows for the transient translocation of NF-κB into the nucleus (23) and binding to DNA. The activation of NF-κB plays a pivotal role in the regulation of diverse cellular processes such as inflammation, immune response, differentiation, proliferation, and apoptosis (22).

We hypothesized that NF-κB may be a downstream target of the CCR7 pathway induced by CCL19. The goals of this study were as follows: to determine whether NF-κB is activated by CCR7 through PI3K/Akt/mTOR and to identify the signal cascade's role in head and neck squamous cell survival as well as in the development and progression of cancer.

Materials and methods

Human tumor samples and cell lines. SCCHN tissue specimens were obtained from 78 patients by biopsy prior to chemotherapy or radiotherapy at the Department of Oral and Maxillofacial Surgery, School and Hospital of Stomatology, China Medical University. The term 'metastatic' in this study refers to patients with positive lymph nodes that were recognized either at initial presentation or later based on the histopathological diagnosis after neck dissection. The classification of SCCHN, including primary tumors (T), regional lymph nodes (N), distant metastasis (M) and stage grouping, was determined according to the rules of the International Union Against Cancer (UICC) for Head and Neck Cancer (Tumor node metastasis, TNM classification, 1997). Ten samples of normal tissues adjacent to the benign tumor were chosen as controls. Gastric cancer was chosen as positive control sample, and negative control sample was absence of primary antibody. The study protocol was granted approval from the Ethics Committee of the China Medical University, and informed consent was obtained from the patients before surgery.

PCI-4B and PCI-37B, which are well-characterized SCCHN cell lines that are derived from the metastatic lymph node of SCCHN patients, were kindly donated by the University of Pittsburgh Cancer Institute (19,20). The cells were cultured in DMEM medium (Invitrogen, Carlsbad, CA, USA) containing 10% fetal bovine serum (Gibco, Carlsbad, CA, USA), 100 U/ml penicillin G and 100 U/ml streptomycin. When inhibitors were used, we ensured that the dosage used did not affect the viability or expression of CCR7 by the cells.

Reagents and antibodies. CCL19, CCR7 specific monoclonal antibody (mouse antihuman CCR7 antibody) were purchased from R&D System (Minneapolis, MN, USA), PI3K inhibitor (LY294002), Akt inhibitor and mTOR inhibitor (rapamycin) were purchased from Merck-Calbiochem (Darmstadt, Germany), NF-κB inhibitor (PDTC), 3-(4,5-dimethyl-2-tetrazolyl)-2,5-diphenyl-2H tetrazolium bromide (MTT), propidium iodide (PI), 4,6-diamino-2-phenyl indole (DAPI) and dimethyl sulfoxide (DMSO) were purchased from Sigma (St. Louis, MI, USA). Rabbit NF-κB p65 antibody and rabbit phospho-IκBα (serine 32) antibody were purchased from Cell Signaling Technology (Beverly, MA, USA), Annexin-V/PI Apoptosis Detection Kit was purchased from BD Bioscience PharMingen (Rockville, MD, USA). TransAM™ NF-κB p65 assay kit was purchased from Active Motif (Tokyo, Japan).

Immunohistochemical staining and evaluation. Sections were deparaffinized in xylene for 10 min and were then rehydrated through graded alcohols. To inhibit endogenous peroxide activity, sections were immersed in 100% methanol containing 0.3% hydrogen peroxide for 40 min. Following immersion, sections were put in a microwave oven in a jar filled with 10 mM sodium citrate buffer (pH 6.0) for 10 min and cooled at room temperature. Sections were incubated with normal goat serum for 20 min and were then incubated with the primary antibody for 1 h. After the incubation period, sections were washed three times with PBS and were then incubated with the linking reagent (biotinylated anti-immunoglobulin, Zymed, South San Francisco, CA, USA) at room temperature for 1 h. After being washed three times with PBS, the sections were incubated with a complex of avidin DH and biotinlylated enzyme (Zymed) for 30 min. The sections were again washed three times with PBS and incubated with a medium consisting of an equal volume of 0.02% hydrogen peroxide and diaminobenzidine tetrahydrochloride (Zhongshan Ltd., Beijing, China) for 1 min in the dark. After chromogen development, sections were washed in water and counterstained with hematoxylin.

The stained slides were investigated independently by two pathologists who had no knowledge of the clinical parameters and outcomes. All these cells were scored as negative (-) (<10% or no staining), weak postive (+) (11-50%), positive (++) (51-75%), or strongly positive (+++) (>75%).

Western blot analysis. Cells were treated with or without the inhibitors and CCL19 was added following treatment. Cells were harvested in a lysis buffer (10 mM Tris HCl, pH 7.6, 50 mM $Na_4P_2O_7$, 50 mM NaF, 1 mM NaV_3O_4, 1% Triton X-100 and 1X protease inhibitor of protein tyrosine phosphatases). Lysates were sonicated for 3 sec and centrifuged at 4˚C, 14,000 rpm for 30 min. The supernatant was collected for protein quantification using the Bio-Rad Protein Assay dye reagent (Bio-Rad Laboratories, Richmond, CA, USA). Fifty micrograms of protein were size-fractionated through a 10% SDS-PAGE gel and transferred onto nitrocellulose filters. The filters were blocked (1% non-fat dry milk, 0.1% Triton X-100, 150 mM NaCl, 50 mM Tris [tris(hydroxymethyl)aminomethane] (pH 7.5) and incubated with the rabbit phospho-IκBα antibody, which was diluted to a ratio of 1:1000. Nitrocellulose filters were incubated with horseradish peroxidase-conjugated secondary antibodies. Bands were visualized using the enhanced chemiluminescence system (Amersham Pharmacia Biotech, Piscataway, NJ, USA) and quantified by scanning densitometry using FlourChem V2.0 software.

Immunostaining and fluorescence microscopy. Cells were fixed in 4% paraformaldehyde in PBS (10 min at room temperature) and permeabilized with 0.2% Triton X-100

(10 min at room temperature). Cells were then incubated individually in rabbit NF-κB p65 antibody (1 h at room temperature) and FITC-conjugated anti-rabbit immunoglobulins (1 h at room temperature). Cell nuclei were stained by DAPI. Representative fields of cells were photographed by fluorescence microscopy.

TransAM NF-κB p65 transcription factor assay kit. The TransAM NF-κB p65 assay kit, an ELISA-based kit used to detect and quantify transcription factor activation, is specific for bound NF-κB p65. This kit has been shown to be 10 times more sensitive and 40 times faster than the gel retardation technique. Briefly, cells were scraped off the dishes and washed twice with PBS. The nuclear protein was extracted using a nucleic protein extraction kit (Keygen, Nanjing, Jiangsu, China) and quantified by protein quantitation, similar to the quantification process in a Western blot analysis. A 12-μg sample of the nuclear protein from the different samples was added to each of the sample wells. After NF-κB bound to its consensus sequence, the primary antibody and secondary antibody were added individually to the sample wells. Each well was incubated for 1 h at room temperature with mild agitation (100 rpm on a rocking platform) and was then exposed to a colorimetric reaction using a developing solution. The optical density (OD), which represented NF-κB constitutive activation, was detected within 5 min by a spectrophotometer (Tecan, Männedorf, Switzerland) at 450 nm with a reference wavelength of 655 nm. The NF-κB DNA-binding activity was calculated relative to the control group (untreated group).

MTT assay. This is a colorimeter assay that relies on the ability of viable cells to convert a soluble tetrazolium salt, MTT, into a quantifiable, insoluble formazan precipitate (yellow to purple color change). Cell death correlates with reduced purple precipitate formation. In brief, SCCHN cells were plated in a 96-well plate at an initial density of $5x10^4$ cells per well. Confluent cells (70-80%) were serum starved for 24 h, then treated with or without the inhibitors, followed by the addition of CCL19, and then cisplatin. Media were discarded and 20 μl MTT (5 μg/ml in PBS) was added for 4 h. DMSO (200 μl) was then added to each well, and the plate was incubated at 37˚C in 5% CO_2 atmosphere for 1 h to lyse all of the cells, and the media were collected for measurement. OD was read by a spectrometer (Tecan) at 490 nm. The percent cell viability was calculated as follows: viability percentage (%) = (OD of treatment group)/(OD of control group) x 100%.

Flow cytometry. To determine the role of CCR7 and the signaling pathway in apoptosis, Annexin-V and PI staining were performed. Briefly, cells were pretreated with the inhibitors, followed by the addition of CCL19, and then cisplatin. Cells were harvested at the indicated time points, and the cells were stained with fluorescein isothiocyanate (FITC)-conjugated Annexin V and PI according to the manufacturer's recommendation. In these experiments, the cells that were apoptotic were those that are Annexin-V positive/PI negative. Samples were analyzed using a FACSCalibur flow cytometer and CellQuest software (BD, Sparks, MD, USA).

For cell cycle analysis, cells were treated the same way as they were in the apoptosis assay. Cells were harvested and fixed in 70% ethyl alcohol for 16 h and stained with a cocktail of PI (50 μg/ml), RNAase (20 μg/ml) and sodium citrate (1 mg/ml) in the dark at 4˚C for at least 20 min. Samples were analyzed using a FACSCalibur flow cytometer and CellQuest software (BD).

Statistical analysis. Data were expressed as the mean ± standard deviation (SD) of repeated assays. The association between CCR7 or NF-κB expression and clinicopathological factors were analyzed using a χ^2 test. Statistical differences between the two groups were evaluated using an unpaired Student's t-test. P-values <0.05 were considered to be significant. All statistical analyses were performed with the software SPSS 11.0.

Results

Correlations between CCR7, NF-κB expression and clinicopathological factors. First, we studied the expression of CCR7 and NF-κB-signaling molecules in specimens from SCCHN patients by immunohistochemical staining. As Fig. 1 shows, CCR7 was strongly immunolocalized in the membrane and the cytoplasm of cancer cells, and NF-κB was detected mostly in the cytoplasm and also in the nucleus. Of the 78 patients, 48 cases were positive for CCR7 (48/78), and 38 cases were positive for NF-κB (38/78). However, in ten control cases, only one case was positive for CCR7 (1/10) and no cases were positive for NF-κB (0/10). The differences between SCCHN and normal tissues in the two molecules were significant (P<0.05). Table I summarizes the relationship between CCR7 expression, NF-κB expression and the clinicopathological factors of the 78 SCCHN patients. The expression of CCR7 and NF-κB were both significantly correlated with cervical lymph node metastasis and clinical stage (P<0.05). However, there were no significant differences between CCR7 or NF-κB expression and age or gender. Of the 78 cases, 28 cases were $CCR7^+/NF\text{-}\kappa B^+$, and 20 cases were $CCR7^-/NF\text{-}\kappa B^-$, which suggests that the two molecules were also correlated with each other (Spearman r=0.414, P<0.05). In addition, in metastatic tumors, the level of CCR7 and NF-κB were all seem higher than that of the primary tumor (Fig. 1).

CCL19-induced phosphorylation of IκBα through PI3K/Akt. Phosphorylation of IκBα by upstream kinases promotes its degradation, allowing NF-κB to translocate to the nucleus and induce target genes. Therefore, the level of phosphorylation of IκBα can represent the constitutive activation of NF-κB. We hypothesized that NF-κB is a nuclear target in the CCL19-induced survival via a PI3K/Akt cascade in metastatic SCCHN cells. To study this, we determined whether CCL19 induces phosphorylation of IκBα. Cells were treated with CCL19 for the indicated time and were used to prepare lysates that were analyzed by Western blot analysis with anti-phospho-IκBα. The results showed that CCL19-stimulated PCI-4B and PCI-37B cells showed a significant increase in the phosphorylation of IκBα at serine 32, and that this phosphorylation was time-dependent within 60 min.

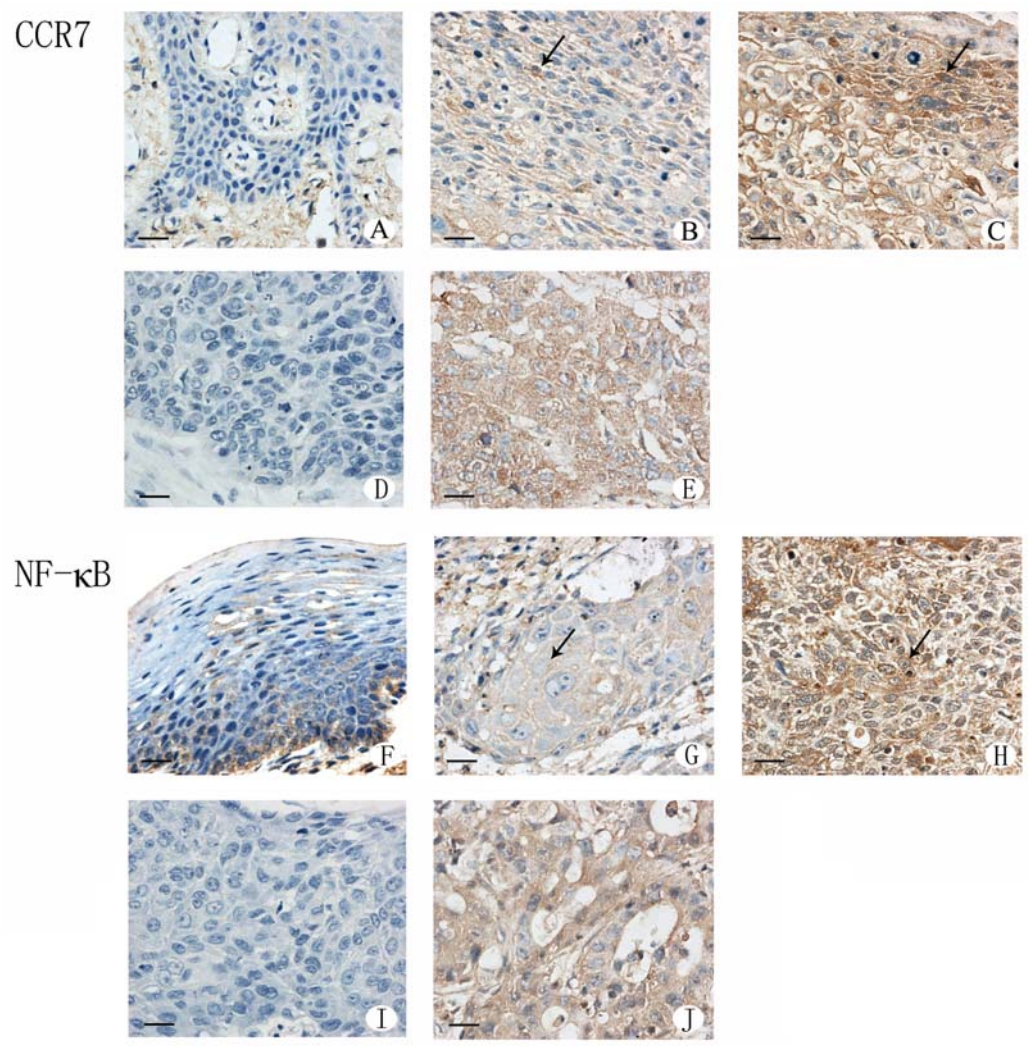

Figure 1. Immunohistochemical staining of CCR7 and NF-κB in normal tissues, primary SCCHN, and metastatic lymph nodes (x400). (A and F) Negative staining of CCR7 or NF-κB in a normal tissue. (B and G) Positive staining of CCR7 or NF-κB in primary SCCHN. (C and H) Strong positive staining of CCR7 or NF-κB in a metastatic lymph node. (D and I) No staining of CCR7 or NF-κB in negative control samples (absence of primary antibody). (E and J) Strong positive staining of CCR7 or NF-κB in positive control sample (gastric cancer). Arrow indicates CCR7 or NF-κB positive cells (yellow-staining). Bar, 100 μm.

In 120 min, the phosphorylation was approximately equal to that observed in 60 min (Fig. 2). To study whether this phosphorylation is induced by the CCR7 activation via a PI3K/Akt/mTOR cascade, the CCR7 mAb, PI3K inhibitor (LY294002), Akt inhibitor and mTOR inhibitor (rapamycin) were pretreated before treatment with CCL19. As shown in Fig. 3, the inhibitors can attenuate the phosphorylation of IκBα to varying degrees, indicating that NF-κB may be a nuclear target of CCR7 via the PI3K/Akt/mTOR cascade. Fig. 3 also shows that factors inhibiting NF-κB activation (PDTC) could also attenuate the phosphorylation of IκBα.

Generally, NF-κB exists in an inactive form in the cytoplasm. When IκBs are phosphorylated, NF-κB translocates to the nucleus. Thus, determining whether NF-κB exhibits nucleus translocation can be used to determine whether or not it is active. In Fig. 4, NF-κB was labeled by FITC, which appears green under a fluorescence microscope, and the nucleus was stained by DAPI, which appears blue under a fluorescence microscope. In untreated PCI-4B cells, NF-κB is distributed evenly in the cytoplasm and nucleus. After treatment with CCL19, the majority of NF-κB was observed to be aggregated in the nucleus, appearing as regions of intensive fluorescence while the cytoplasm appeared to be weakly fluorescent. After being pretreated by CCR7 mAb and PDTC, respectively, the intensity of fluorescence of NF-κB in the nucleus decreased significantly and the cytoplasm and nucleus recovered to become well-distributed. The same results were observed in PCI-37B cells.

After NF-κB was translocated into the nucleus, it bound with DNA and activated target genes that regulate a number of cellular processes. To study the DNA-binding capacity of NF-κB in the nucleus, a TransAM NF-κB p65 transcription factor assay kit was used. As shown in Fig. 5, CCL19 induced the activation of NF-κB, such that NF-κB was more than twice as high as the baseline (incubation in media alone) in both cell lines. This DNA-binding capacity was also blocked selectively in the presence of CCR7 mAb, LY294002, Akt inhibitor and rapamycin, as well as in the presence of PDTC. Taken together, these results showed that NF-κB is a nuclear target of the CCL19-induced CCR7

Table I. Correlations between CCR7, NF-κB expression and clinicopathological factors of SCCHN.

Clinicopathological characteristics	No. of cases	CCR7		Statistical analysis	NF-κB		Statistical analysis
		+-+++	-		+-+++	-	
Age							
≥60	40	25	15	χ^2=0.032	21	19	χ^2=0.470
<60	38	23	15		17	21	
Gender							
Male	50	32	18	χ^2=0.357	27	23	χ^2=1.555
Female	28	16	12		11	17	
Tumor size							
T1, T2	65	37	28	χ^2=3.510	28	37	χ^2=4.967[a]
T3, T4	13	11	2		10	3	
Clinical stage							
I, II	37	15	22	χ^2=13.113[a]	7	30	χ^2=25.019[a]
III, IV	41	33	8		31	10	
Nodal metastasis							
Yes	37	29	8	χ^2=8.434[a]	28	9	χ^2=20.475[a]
No	41	19	22		10	31	

[a]P<0.05 (the internal difference of CCR7 or NF-κB expression within clinicopathological characteristics).

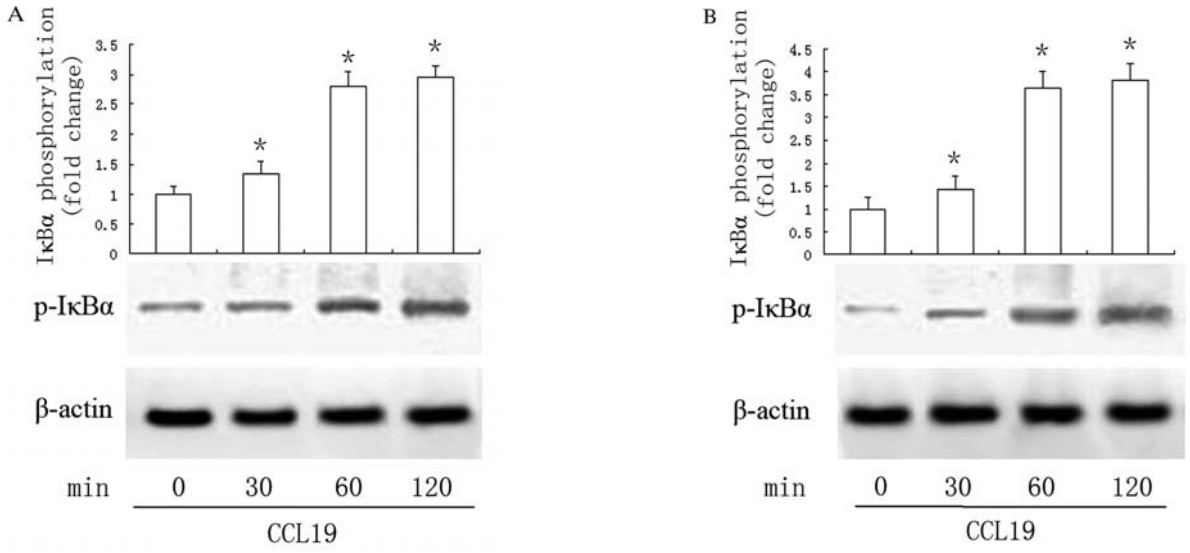

Figure 2. CCL19 induces the phosphorylation of IκBα. PCI-4B (A) and PCI-37B cells (B) were treated with CCL19 (200 ng/ml, at 37˚C for 30-120 min) and were then analyzed to determine the level of phosphorylation of IκBα by Western blotting. The relative mean density of p-IκBα was calculated relative to control group (CCL19, 0 min), and ß-actin was used as an internal control. The results are representative of three independent experiments. *Indicates P<0.05 in comparison to the control group.

signaling pathway in metastatic SCCHN cells, and that this pathway occurs via the PI3K/Akt/mTOR cascade.

NF-κB is involved in the signaling pathway of CCR7, which protects cells from cisplatin-induced death. CCR7 can regulate SCCHN cell survival (19,20). Our previous studies also showed that PI3K/Akt/mTOR participates in this mechanism. Since NF-κB has many different functions in a number of different cell types, whether it also participate this mechanism in the downstream of CCR7 in SCCHN cell lines? To study this, we examined the viability, cell-cycle and apoptosis of the two cell lines. As shown in Table II, the percentage of viable cells upon cisplatin treatment was reduced to <50 from 100% in untreated PCI-4B and PCI-37B

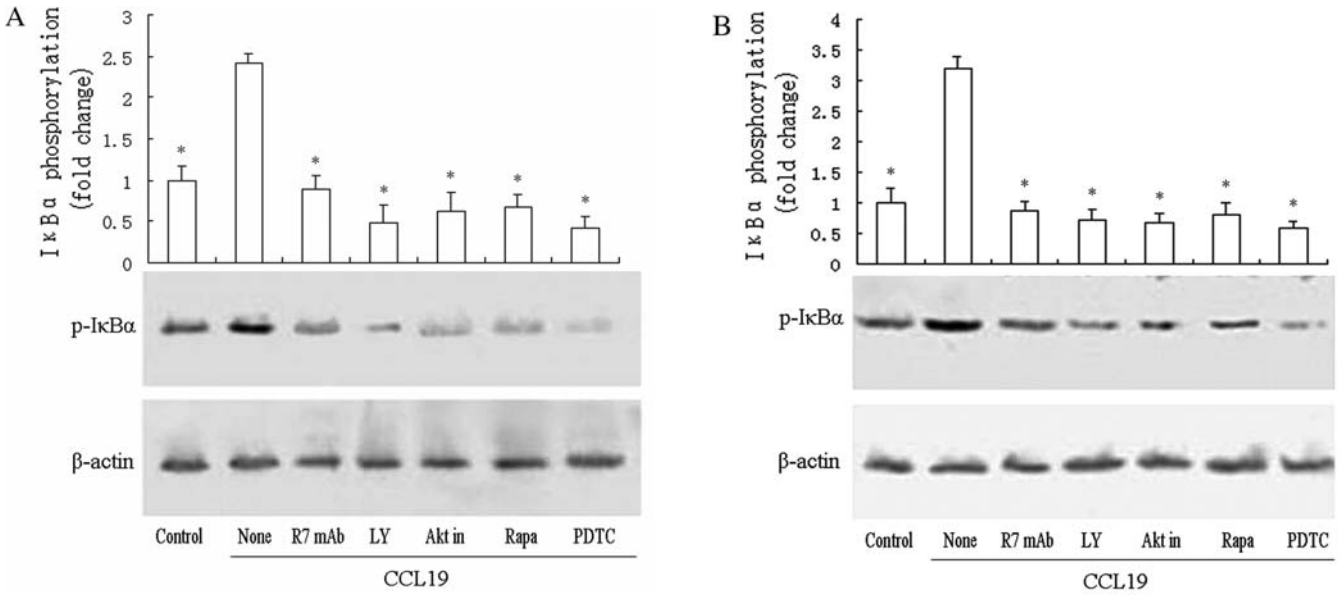

Figure 3. CCR7-induced phosphorylation of IκBα via the PI3K/Akt/mTOR pathway. PCI-4B (A) and PCI-37B cells (B) were pretreated with or without CCR7 mAb (R7 mAb, 10 μg/ml), LY294002 (LY, 10 μM), Akt inhibitor (Akt in, 10 μM), rapamycin (Rapa, 100 nM) and PDTC (50 μM) at 37˚C for 4 h, followed by treatment with CCL19 (200 ng/ml) at 37˚C for 1 h. Cell lysates were then analyzed for the presence of phosphorylated IκBα by Western blotting. The relative mean density of p-IκBα was calculated relative to the control group (the untreated group). ß-actin was used as an internal control. The results are representative of three independent experiments. *Indicates P<0.05 compared to the CCL19 group.

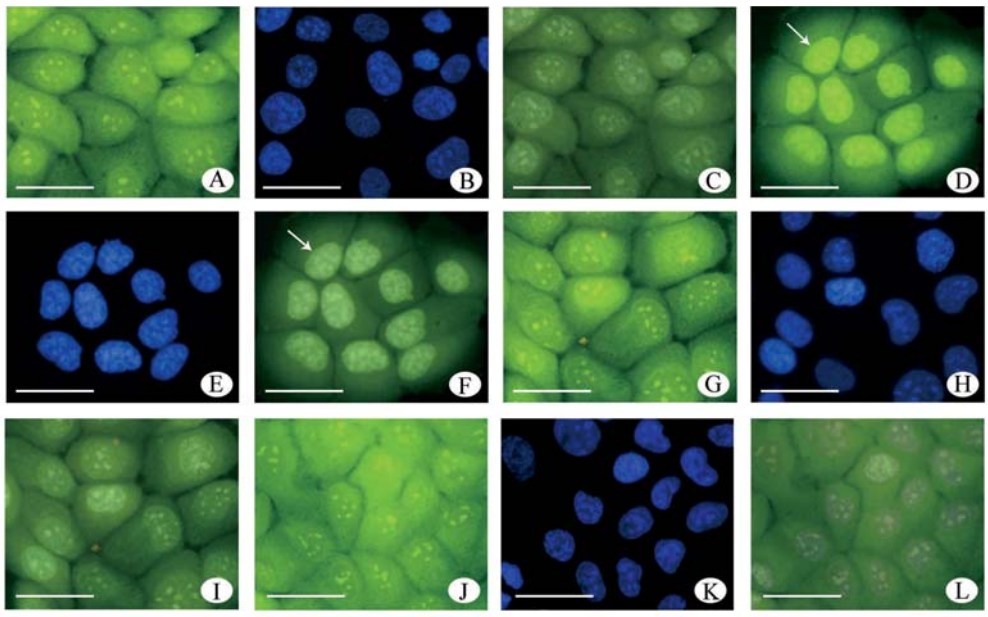

Figure 4. CCR7-induced nucleus translocation of NF-κB. PCI-4B cells were pretreated with or without CCR7 mAb (10 μg/ml) or PDTC (50 μM) at 37˚C for 4 h, followed by treatment with CCL19 (400 ng/ml) at 37˚C for 6 h. The location of NF-κB (p65) in the cells was then examined by immunostaining and fluorescence microscopy. (A) NF-κB labeled by FITC (green fluorescence) in untreated cells. (B) Nucleus stained by DAPI (blue fluorescence) in untreated cells. (C) Overlap of NF-κB (green fluorescence) and nucleus (blue fluorescence) in untreated cells. (D) NF-κB labeled by FITC (green fluorescence) in CCL19-treated cells. (E) Nucleus stained by DAPI (blue fluorescence) in CCL19-treated cells. (F) Overlap of NF-κB (green fluorescence) and the nucleus (blue fluorescence) in CCL19-treated cells. (G) NF-κB labeled by FITC (green fluorescence) in CCL19+CCR7 mAb-treated cells. (H) Nucleus stained by DAPI (blue fluorescence) in CCL19+CCR7 mAb-treated cells. (I) Overlap of NF-κB (green fluorescence) and nucleus (blue fluorescence) in CCL19+CCR7 mAb-treated cells. (J) NF-κB labeled by FITC (green fluorescence) in CCL19+PDTC-treated cells. (K) Nucleus stained by DAPI (blue fluorescence) in CCL19+PDTC-treated cells. (L) Overlap of NF-κB (green fluorescence) and nucleus (blue fluorescence) in CCL19+PDTC-treated cells. Arrow indicates positive staining of NF-κB in nucleus. Bar, 100 μm.

cells. However, when CCL19 was added, the viability increased to ~80%. The effect of cisplatin and CCL19 on the G_1 phase and on apoptosis were consistent with their effects on viability. This data showed that CCR7 regulates SCCHN cell survival. To investigate the role of NF-κB in this pathway, we used cisplatin to induce death and CCL19 to protect the cells. Then, we analyzed changes in cell viability, cell cycle progression and apoptosis in the presence of the inhibitors of

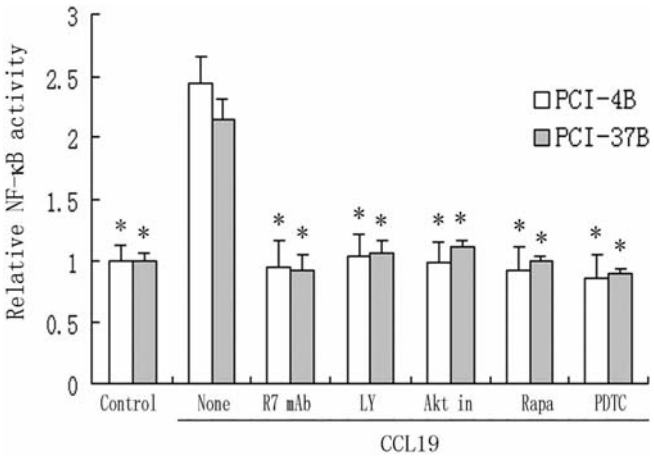

Figure 5. CCR7-induced DNA-binding capacity of NF-κB via the PI3K/Akt/mTOR pathway. PCI-4B and PCI-37B cells were pretreated with or without CCR7 mAb (R7 mAb, 10 μg/ml), LY294002 (LY, 10 μM), Akt inhibitor (Akt in, 10 μM), rapamycin (Rapa, 100 nM) and PDTC (50 μM) at 37˚C for 4 h, followed by treatment with CCL19 (200 ng/ml) at 37˚C for 1 h. The NF-κB DNA-binding activity was then examined using a TransAM NF-κB p65 Transcription Factor Assay Kit. The results are representative of three independent experiments. *Indicates P<0.05 compared to the CCL19 group.

this pathway. As shown in Table II, PDTC blocked the effect of CCL19 and CCR7 in both cell lines, leading to decreased cell viability, an increased percentage of cells in the G_1 phase and an increase in the number of cells undergoing apoptosis. The difference between cells pretreated with PDTC and cells that were only treated with CCL19 and cisplatin was significant, as well as LY294002, Akt inhibitor and rapamycin, indicating that NF-κB participates in CCR7-induced activation of the PI3K/Akt/mTOR pathway to mediate cell survival.

Discussion

Squamous cell carcinoma is the most common malignant tumor occurring in the head and neck and has a poor prognosis. CCR7 has been shown to interact with chemokines such as CCL19 and CCL21, to enhance the survival and proliferation of metastatic SCCHN cells (19,20). However, it is unclear how CCR7 protects cells and what intercellular signaling pathways are involved. We determined that NF-κB is an important nuclear target of the CCR7 signaling pathway via the PI3K/Akt/mTOR cascade in metastatic SCCHN cells. This pathway can serve to reverse cell death, and is correlated with the development and progression of cancer.

The activation of NF-κB may result from different signaling pathways triggered by a variety of cytokines, growth factors and tyrosine kinases. Enhanced expression of members of the epidermal growth factor receptor, the insulin growth factor receptor, and the tumor necrosis factor receptor families may also be responsible for NF-κB activation (24). In SCCHN cell lines, our results showed that stimulation of CCL19 could also result in an elevation in IκBα phosphorylation at Serine 32, which causes NF-κB to translocate into the nucleus and bind to DNA. CCL19 can activate downstream mediators of CCR7, including Akt in metastatic SCCHN cells (19). The activated Akt molecules directly phosphorylate TSC1 (tuberous sclerosis complex 1) and TSC2 (tuberous sclerosis complex 2). Since these are negative regulators of mTOR, the loss of TSC1 or TSC2 leads to the hyperactivation of mTOR signaling (25). It is generally accepted that PI3K/Akt is involved in NF-κB activation (24,26). Regarding the relationship between mTOR and NF-κB, Jundt *et al* reported that, in Hodgkin's lymphoma (HL) and anaplastic large cell lymphoma (ALCL), the mTOR signaling pathway inhibitor (RAD) can also significantly down-regulate constitutive NF-κB DNA binding activity. This inhibits the proliferation

Table II. The percentage of cells that were viable, in the G_1 phase or undergoing apoptosis, respectively, after treatment with inhibitors, CCL19 and cisplatin.

	Viability (%)		G_1 phase (%)		Apoptosis (%)	
	4B	37B	4B	37B	4B	37B
Untreated	100±0.00	100±0.00	65.98±2.86	70.75±2.05	4.04±0.92	2.31±0.71
Cisplatin	45.33±2.26[a]	42.94±3.27[a]	88.65±1.43[a]	89.41±1.79[a]	18.35±1.91[a]	15.01±0.84[a]
CCL19+cisplatin	82.90±3.52	80.45±5.67	72.14±2.66	76.39±1.45	9.59±0.86	7.55±0.66
CCR7 mAb+CCL19+cisplatin	58.80±2.85[a]	57.89±5.23[a]	82.40±2.14[a]	83.15±1.67[a]	14.90±0.36[a]	11.26±0.71[a]
LY294002+CCL19+cisplatin	53.63±3.80[a]	53.05±3.92[a]	83.40±1.77[a]	88.05±1.81[a]	14.49±1.46[a]	12.67±0.77[a]
Akt inhibitor+CCL19+cisplatin	60.97±6.07[a]	65.83±2.27[a,b]	82.56±2.14[a]	83.05±1.25[a]	13.21±1.15[a]	10.89±0.71[a]
Rapamycin+CCL19+cisplatin	60.40±1.67[a]	61.32±3.09[a,b]	89.21±2.49[a]	88.38±2.13[a]	14.91±1.19[a]	10.56±0.90[a]
PDTC+CCL19+cisplatin	46.63±3.95[a]	38.26±4.36[a]	88.08±1.99[a]	87.51±0.89[a]	15.71±0.72[a]	15.30±0.56[a]

PCI-4B and PCI-37B cells were pretreated with or without the following: CCR7 mAb (10 μg/ml); PI3K inhibitor (LY294002, 100 μM); Akt inhibitor (100 μM); mTOR inhibitor (rapamycin, 1 μM); and PDTC (50 μM) at 37˚C for 4 h. Following treatment, cells were treated with CCL19 (400 ng/ml) at 37˚C for 6 h, and then with cisplatin (80 μM in MTT assay and 40 μM in Annexin-V/PI staining and PI staining) at 37˚C for 12 h. The percentage of cells that were viable, in the G_1 phase and undergoing apoptosis, respectively, were assayed using an MTT assay, Annexin-V/PI staining and PI staining. The data are shown as the mean ± SD of three independent experiments. [a]Indicates P<0.01 compared to the CCL19+cisplatin group; [b]indicates P<0.05 compared to the CCL19+cisplatin group.

of cells *in vitro* and arrests cell cycle progression in G_0/G_1 (27). In the human lung cancer cell line A549, IL-1ß up-regulates functional NF-κB through a classical inflammatory signaling pathway involving PI3K/Akt/mTOR (28). The same result was seen in B6.Sle1b^z.lpr mice (29). In human solid tumors, the reports are rare. Our results showed that when CCR7 and the PI3K/Akt/mTOR pathway were inhibited, the CCL19-induced NF-κB activation was also inhibited, IκBα phosphorylation decreased and less NF-κB translocated into the nucleus and bound to DNA. Thus, in SCCHN, CCR7-mediated NF-κB activation occurred not only via PI3K/Akt but also via their downstream mTOR.

CCR7 protects metastatic SCCHN cells from cell death via PI3K/Akt/mTOR (21). NF-κB plays a pivotal role in the regulation of a number of cellular processes, such as inflammation, immune response, differentiation, proliferation, and apoptosis (22). To investigate the role of NF-κB in the CCR7 pathway in metastatic SCCHN cells, we assayed cell viability, the percent of cells in the G_1 phase and the percent of cells undergoing apoptosis. The results showed that when PI3K/Akt/mTOR and NF-κB were blocked, viability decreased and an increased percentage of cells stayed in G_1 phase and began to undergo apoptosis, despite the stimulation by CCL19. This indicates that NF-κB may be a nuclear target in the CCR7-mediated protection of metastatic SCCHN cells against death via the PI3K/Akt/mTOR cascade.

CCR7 and NF-κB were highly expressed in various tumors, including SCCHN (30-33). The results from our 78 cases were consistent with previous studies. CCR7 and NF-κB expression were all significantly correlated with cervical lymph node metastasis and clinical stage. Our results also demonstrated the correlation between CCR7 and NF-κB. Following our results *in vitro*, together with the results of other studies (20,21,34-36), we presumed that in SCCHN CCR7-induced NF-κB activation, the high CCR7 and NF-κB expression regulates cell survival and promotes tumor cells to metastasize to lymph nodes in the concentration gradient of chemokine. Once arriving at the lymph node, the expression of CCR7 and NF-κB was enhanced conversely. These processes were mediated by PI3K/Akt/mTOR.

Some mediated survival mechanisms exist in malignant tumors, and it is necessary to decode this aspect of the behavior of cancer in order to develop more effective and less toxic therapies. Our experiments demonstrated that CCR7-dependent activation of PI3K/Akt/mTOR and NF-κB participates in this mechanism. However, the PI3K signaling pathway is not a linear pathway, but a result of integrated signals leading to complex cellular responses. Similarly, CCR7-mediated activation of this pathway is complex. Therefore, it is impossible to cure tumors by simply blocking the CCR7 or NF-κB pathway. However, our data provided a new idea to improve prognosis by blocking CCR7 and NF-κB in cooperation with other factors as an adjuvant treatment of chemotherapy or surgery. Therefore, further work on this topic should be conducted.

Acknowledgements

The authors thank Jie Liu for her excellent technical assistance in cell culture. This research was supported by a grant from the National Natural Science Foundation of China (No. 30672331) and Foundation of Liaoning Educational Commission (No. 2009A755).

References

1. Butcher EC, Williams M, Youngman K, Rott L and Briskin M: Lymphocyte trafficking and regional immunity. Adv Immunol 72: 209-253, 1999.
2. Campbell JJ and Butcher EC: Chemokines in tissue-specific and microenvironment-specific lymphocyte homing. Curr Opin Immunol 12: 336-341, 2000.
3. Morales J, Homey B, Vicari AP, *et al*: CTACK, a skin-associated chemokine that preferentially attracts skin-homing memory T cells. Proc Natl Acad Sci USA 96: 14470-14475, 1999.
4. Zlotnik A and Yoshie O: Chemokines: a new classification system and their role in immunity. Immunity 12: 121-127, 2000.
5. Nagira M, Imai T, Yoshida R, *et al*: A lymphocyte-specific CC chemokine, secondary lymphoid tissue chemokine (SLC), is a highly efficient chemoattractant for B cells and activated T cells. Eur J Immunol 28: 1516-1523, 1998.
6. Ding Y, Shimada Y, Maeda M, *et al*: Association of CC chemokine receptor 7 with lymph node metastasis of esophageal squamous cell carcinoma. Clin Cancer Res 9: 3406-3412, 2003.
7. Takanami I: Overexpression of CCR7 mRNA in non-small cell lung cancer: correlation with lymph node metastasis. Int J Cancer 105: 186-189, 2003.
8. Murakami T, Cardones AR and Hwang ST: Chemokine receptors and melanoma metastasis. J Dermatol Sci 36: 71-78, 2004.
9. Iijima N, Yanagawa Y, Clingan JM and Onoe K: CCR7-mediated c-Jun N-terminal kinase activation regulates cell migration in mature dendritic cells. Int Immunol 17: 1201-1212, 2005.
10. Gunther K, Leier J, Henning G, *et al*: Prediction of lymph node metastasis in colorectal carcinoma by expression of chemokine receptor CCR7. Int J Cancer 116: 726-733, 2005.
11. Cabioglu N, Yazici MS, Arun B, *et al*: CCR7 and CXCR4 as novel biomarkers predicting axillary lymph node metastasis in T1 breast cancer. Clin Cancer Res 11: 5686-5693, 2005.
12. Schimanski CC, Bahre R, Gockel I, *et al*: Chemokine receptor CCR7 enhances intrahepatic and lymphatic dissemination of human hepatocellular cancer. Oncol Rep 16: 109-113, 2006.
13. Banas B, Wornle M, Berger T, *et al*: Roles of SLC/CCL21 and CCR7 in human kidney for mesangial proliferation, migration, apoptosis, and tissue homeostasis. J Immunol 168: 4301-4307, 2002.
14. Banas B, Wornle M, Merkle M, *et al*: Binding of the chemokine SLC/CCL21 to its receptor CCR7 increases adhesive properties of human mesangial cells. Kidney Int 66: 2256-2263, 2004.
15. Wornle M, Schmid H, Merkle M and Banas B: Effects of chemokines on proliferation and apoptosis of human mesangial cells. BMC Nephrol 5: 8, 2004.
16. Sanchez-Sanchez N, Riol-Blanco L, de la Rosa G, *et al*: Chemokine receptor CCR7 induces intracellular signaling that inhibits apoptosis of mature dendritic cells. Blood 104: 619-625, 2004.
17. Kim JW, Ferris RL and Whiteside TL: Chemokine C receptor 7 expression and protection of circulating $CD8^+$ T lymphocytes from apoptosis. Clin Cancer Res 11: 7901-7910, 2005.
18. Liu FY, Zhao ZJ, Li P, Ding X and Sun CF: The effect of CCL19 on the viability of head and neck squamous cancer cells. Shanghai Kou Qiang Yi Xue 19: 158-161, 2010.
19. Wang J, Zhang X, Thomas SM, *et al*: Chemokine receptor 7 activates phosphoinositide-3 kinase-mediated invasive and prosurvival pathways in head and neck cancer cells independent of EGFR. Oncogene 24: 5897-5904, 2005.
20. Mburu YK, Wang J, Wood MA, Walker WH and Ferris RL: CCR7 mediates inflammation-associated tumor progression. Immunol Res 36: 61-72, 2006.
21. Liu FY, Zhao ZJ, Li P, Ding X, Zong ZH and Sun CF: Mammalian target of rapamycin (mTOR) is involved in the survival of cells mediated by chemokine receptor 7 through PI3K/Akt in metastatic squamous cell carcinoma of the head and neck. Br J Oral Maxillofac Surg 48: 291-296, 2009.
22. Krappmann D, Wegener E, Sunami Y, *et al*: The IkappaB kinase complex and NF-kappaB act as master regulators of lipopolysaccharide-induced gene expression and control subordinate activation of AP-1. Mol Cell Biol 24: 6488-6500, 2004.

23. Verma IM, Stevenson JK, Schwarz EM, Van Antwerp D and Miyamoto S: Rel/NF-kappa B/I kappa B family: intimate tales of association and dissociation. Genes Dev 9: 2723-2735, 1995.
24. Dolcet X, Llobet D, Pallares J and Matias-Guiu X: NF-kB in development and progression of human cancer. Virchows Arch 446: 475-482, 2005.
25. Wang X and Proud CG: The mTOR pathway in the control of protein synthesis. Physiology (Bethesda) 21: 362-369, 2006.
26. Saitoh M, Ohmichi M, Takahashi K, *et al*: Medroxyprogesterone acetate induces cell proliferation through up-regulation of cyclin D1 expression via phosphatidylinositol 3-kinase/Akt/nuclear factor-kappaB cascade in human breast cancer cells. Endocrinology 146: 4917-4925, 2005.
27. Jundt F, Raetzel N, Muller C, *et al*: A rapamycin derivative (everolimus) controls proliferation through down-regulation of truncated CCAAT enhancer binding protein {beta} and NF-{kappa}B activity in Hodgkin and anaplastic large cell lymphomas. Blood 106: 1801-1807, 2005.
28. Jung YJ, Isaacs JS, Lee S, Trepel J and Neckers L: IL-1beta-mediated up-regulation of HIF-1alpha via an NFkappaB/COX-2 pathway identifies HIF-1 as a critical link between inflammation and oncogenesis. FASEB J 17: 2115-2117, 2003.
29. Xie C, Patel R, Wu T, *et al*: PI3K/AKT/mTOR hypersignaling in autoimmune lymphoproliferative disease engendered by the epistatic interplay of Sle1b and FASlpr. Int Immunol 19: 509-522, 2007.
30. Nakayama H, Ikebe T, Beppu M and Shirasuna K: High expression levels of nuclear factor kappaB, IkappaB kinase alpha and Akt kinase in squamous cell carcinoma of the oral cavity. Cancer 92: 3037-3044, 2001.
31. Mashino K, Sadanaga N, Yamaguchi H, *et al*: Expression of chemokine receptor CCR7 is associated with lymph node metastasis of gastric carcinoma. Cancer Res 62: 2937-2941, 2002.
32. Seo SI, Song SY, Kang MR, *et al*: Immunohistochemical analysis of NF-kappaB signaling proteins IKKepsilon, p50/p105, p52/p100 and RelA in prostate cancers. APMIS 117: 623-628, 2009.
33. Shang ZJ, Liu K and Shao Z: Expression of chemokine receptor CCR7 is associated with cervical lymph node metastasis of oral squamous cell carcinoma. Oral Oncol 45: 480-485, 2009.
34. Wang J, Xi L, Hunt JL, *et al*: Expression pattern of chemokine receptor 6 (CCR6) and CCR7 in squamous cell carcinoma of the head and neck identifies a novel metastatic phenotype. Cancer Res 64: 1861-1866, 2004.
35. Liu FY, Zhao ZJ, Huang Sh and CF S: Role of PDTC in CCL19 regulating human head and neck squamous cancer cells survival. J China Med Univ 37: 847-849, 2008.
36. Zhao ZJ, Liu FY and Sun CF: Effect of chemokine receptor 7 small interfering RNA on proliferation and invasion of squamous cell carcinoma of head and neck. Zhonghua Kou Qiang Yi Xue Za Zhi 44: 5-10, 2009.